KW

MET O 11 TECHNICAL NOTE NO 228

INVESTIGATIONS OF BALANCE IN THE OPERATIONAL GLOBAL MODEL WITH NORMAL MODE INITIALIZATION

by

Bruce Macpherson

April 1986

Met O 11 (Forecasting Research)
Meteorological Office
London Road
Bracknell
Berkshire RG12 2SZ

Contents

1. Introduction

Normal mode initialization (NMI) is a technique for the elimination of high frequency gravity waves from forecast models, pioneered by Machenhauer, Baer and Tribbia. (For a review see Daley, 1981). NMI ensures that the initial mass and wind fields are in balance so that large amplitude gravity waves are not excited. It is based on a frequency separation of analysed fields into two components: low frequency Rossby modes which we wish to retain and high frequency gravity waves which we seek to remove.

In the operational global model, the alternative method is used of dynamic initialization by repeated insertion with divergence damping to help reduce gravity wave activity (Bell, 1985). In this report, the balance achieved by NMI is compared with that produced by the operational assimilation. In the first section, the impact of NMI on data quality control is assessed. This is followed by an investigation of oscillations in jet streams. Brief consideration is then given to the magnitude of changes made by NMI to an operational analysis. Next, the values of a balance measure in normal mode space are discussed. Here the effectiveness of the operational assimilation is tested against NMI and an early method of dynamic initialization. Finally, in an appendix, the basic principles behind NMI are discussed from a computational view point. NMI has also recently been applied to the global model in a study of the noise present in the regional fine mesh model, which receives its boundary information from the global model. These tests are described by Dickinson and Gange (1985).

2. Balance for Quality Control

2.1 Introduction

A possible role for normal mode initialization in the operational suite is at the data quality control step, when new observations are compared with a first guess field produced by a 6 hour forecast from the previous analysis. As noted by Temperton and Williamson (1981), it is important that the first guess fields are not contaminated with spurious oscillations. Otherwise the risk exists of accepting bad data or rejecting good data. The removal of oscillations from the forecast offers scope for improving the first guess fields and hence the next analysis, especially in data-sparse areas.

The question investigated here is whether the suppression by divergence damping of noise from the repeated insertion method of assimilation is adequate for effective quality control. In a short period like 6 hours, this may not be so.

The issue was examined by comparing the rms fit to observations of background fields derived from operational and initialized analyses. Quality control decisions were also compared. Two cases were chosen at random: 12Z, 15/1/85 and 12Z, 10/5/85. The single observation dataset chosen to compare against the two different background fields was either that selected by the operational quality control run or that by the initialized run. The conclusions drawn were not influenced by this choice.

2.2 Data Flagging

In the 10/5/85 case there was a total of 66 differences in flagging between the operational and initialized runs. There were 3 differences in p_* flagging (near mountains), 20 in temperature, 9 in wind flagging and 34 in humidity. These may be compared with the total numbers of flags set by the operational quality control for the 4 variables which were 46, 172, 54 and 147 respectively. There were no discernible patterns with respect to latitude or pressure level in the data rejected in the control run and accepted in the initialized run or vice versa.

2.3 RMS fit to observations

These results are classified by variable, observation type, pressure level and latitude band. (The mean fit to observations was also examined but showed nothing of particular interest not exhibited by the rms figures). The number of iterations, n_i, used in the nonlinear initialization was also varied between 1 and 3. The number of vertical modes initialized was always 5. (A brief description of the iterative nature of NMI is given in the Appendix).

The effect of NMI was most closely examined for the area 20° - 90°N and n_i = 2. Initialization brought some qualitative improvement in the fitting of surface pressure and temperature at most levels but, for vector wind, caused an increase in rms differences from background. In all cases, though, the quantitative changes were small.

For surface pressure, the maximum improvement was a reduction of 0.2 mb in rms difference for ship observations on 10/5/85. The same reduction was, however, only 0.07 mb on 15/1/85. The small improvements in rms difference from background temperature were less than 0.1 K for radiosonde data and less than 0.4 K for satems. For observation types and levels with very few observations (e.g. 3 Aireps in the range 400-500 mb), the operational background was usually closer to the observations.

The above mentioned increases in rms differences from background wind field with NMI were no larger than 0.6 kt. As such differences lie in the approximate range 8-15 kt, a shift of this magnitude is not very significant. The reason for the poorer fit with initialization is not clear. For wind speed rather than vector wind, NMI brought small improvement in the fit to ship and airep data but was again slightly poorer for other observation types.

Some further aspects may be summarised briefly. Firstly, results for the rms fit to humidity data showed negligible impact. Also, it was mentioned earlier that initialization might have more effect in data-sparse regions. The statistics for surface pressure observations in the area 20° - 90°S were improved with initialization on 15/1/85 but worsened on 10/5/85, the changes in each case being about 0.1 mb. There was a similar lack of definite trend in the fitting of tropical p_* data. One associates oscillations in p_* particularly with the activity of the external mode, so these results tend to confirm the operational assimilation's global suppression of this mode.

In general it was found that initialization with $n_i = 2$ as described above produced more impact than with $n_i = 1$. Statistics with $n_i = 3$ rarely differed from those for $n_i = 2$ except at the third significant figure.

2.4 Discussion

The tests carried out indicate no advantage to be gained from applying NMI to the data quality control process. The operational analyses and first guess fields are therefore well balanced according to this criterion. This is not to say that the initialization has done nothing to improve the balance of the operational analysis.

If one compares the fit of operational and initialized analyses (rather than first guess fields) to the observations, this time the operational analysis is noticeably closer. For example, the rms difference from p_* observations (10/5/85) is smaller by about 0.3 mb in the northern hemisphere and 0.5 mb in the southern hemisphere and tropics than in the initialized analysis. It is likely that the closer fit to data of the operational analysis is achieved at the expense of extra noise generation. Six hours later at the verifying time of the first guess field, this noise evidently does not hamper quality control.

It may be added that the conclusion reached here does not depend on the precise details of the quality control algorithm. Lorenc (private communication) has conducted similar tests on sea surface and coastal synop data with a different Bayesian quality control procedure. His findings match those described here.

3. Balance in Jet Streams

It has been noticed occasionally that model winds in jet streams can undergo a surge or oscillation during the first twelve hours of the forecast. An example of this behaviour is shown in Figure 1. The quantities plotted are spatially averaged over a volume bounded by the levels $\sigma = 0.31$ and $\sigma = 0.19$ of the operational global model and a latitude/longitude area containing the jet stream throughout the forecast period. The oscillations in the u and v wind components are approximately 90° out of phase with each other, indicating that the disturbance is inertial in character. The period of the oscillation in Figure 1 is about 16 hours, close to the inertial period at the latitude of interest.

With NMI as a diagnostic tool, four cases were investigated, the last three of which were picked at random.

1. <u>0Z, 2/6/84</u>

This case was originally singled out by the inability of the coarse mesh model to maintain the strength of the jet. At t+36, the forecast maximum wind was 30 kt lighter than that later analysed. It is the quite separate inertial oscillation up to t+12 (Figure 1), however, that we study here.

Forecasts were made from analyses in which 1, 3 and 5 vertical modes were initialized with either 1, 2 or 3 iterations of NMI. The oscillation is almost completely removed by 1 iteration on 5 modes (Figure 2). Further iterations had negligible impact. It is of interest to know, in linear terms, the relative importance of each mode. Figure 3 provides a rough answer to the effect that all 5 modes are involved to some extent, with no one dominating.

The balance achieved by NMI has resulted in a 5% increase to the mean analysed u component of momentum, with little change to the mean v component. From the height field of Figure 4 and the u wind difference chart of Figure 5, one can see that the increase in u is concentrated on the warm side of the jet to the west of the maximum wind region. Possibly some low airep data was fitted by the model in this region. Barwell and Lorenc (1985) comment on a tendency of the repeated insertion technique to generate unsubstantiated maxima downstream of an observation. There is no evidence here, however, for NMI attempting to shift the jet maximum back upstream.

The effect of NMI on the subsequent forecast can be detected up to about t+9, removing some roughness in the jet core. In the operational run, the maximum wind in the core increases by 10 kt in the first six hours, then falls 18 kt by t+12. In fact this peak is unconnected with the inertial oscillation and is reproduced in the initialized run. The time variation of maximum wind in a region is not a good indicator of balance.

2. <u>6Z, 15/1/85</u>

A strong northerly jet of up to 185 kt in the region 0-20W, 30-60N was investigated. Some evidence of inertial oscillation was found, as seen in the mean kinetic energy (KE) of the jet in Figure 6, though it was not easy to fix the period of the oscillation. In a pure inertial oscillation, the KE is constant. The initialized run produces a steady decline in KE and has a value 7% lower than the operational run at t+6.

3. <u>6Z, 20/7/85</u>

In a jet of maximum strength 150 kt to the west of the UK, an oscillation in the wind field of period about 12 hours was found (Figure 7). One iteration of NMI on 5 vertical modes again removed most of it. The maximum difference in total momentum between operational and initialized runs is about 10% at t+9. Once more initialization increased the mean analysed u component by 5%.

The differences between operational and initialized forecasts were evaluated at t+8. In the u wind field, this revealed that the operational run was up to 14 kt stronger in places (Figure 8). It was more than 5 kt stronger over about half of a 15° latitude by 15° longitude area near the UK. The magnitudes of these differences are lower than typical model errors for t+6 at that latitude of 20 kt at 300 mb. The scale over which the differences exceed 5 kt is, however, comparable to the forecast error correlation scale at t+6. As would be expected, many features of smaller scale are also present in the difference field.

4. <u>6Z, 25/8/85</u>

Over Europe there was a south-westerly jet with maximum wind up to 125 kt. The operational forecast on this occasion showed a smoother evolution of the wind field over the first 12 hours (Figure 9).

The four cases described above show that, on some occasions, the operational analysis has an unbalanced component causing inertial oscillations in jet streams with periods in the range 12-16 hours. These are examples of behaviour noted by Barwell and Lorenc (1985). The repeated insertion assimilation technique with a 6 hour insertion period can preferentially excite modes with period greater than 12 hours.

The oscillations are not present in every forecast but, without a much more detailed examination of the data available to each analysis or a wider variety of case studies, it is difficult to isolate the circumstances in which they occur. It is true, however, that the case showing least imbalance (25/8/85) had the weakest jet core of the four.

The typical errors in mean jet momentum revealed by difference fields of operational and initialized forecasts may be up to 10% at t+9 but little error is visible after t+12.

4. Initialization Increments

Another measure of balance in the operational model is provided by the fields of increments produced when NMI is applied. One might expect the increments to be smaller than those obtained from NMI acting on an analysis which has not undergone any form of dynamic initialization like repeated insertion. It has been noted by several authors (e.g. Williamson & Daley, 1983) that, in the latter case, NMI increments to the analysis can exceed the expected analysis error even over data-rich regions (we do not consider here 'constrained' NMI where the changes can be forced into certain fields rather than others).

Previous reports of NMI increments are mainly of PMSL and 500 mb heights and winds. Linear NMI (see the Appendix) is known to cause very large erroneous increments in the vicinity of steep topography because the normal modes are derived from a basic state without topography. This problem is much reduced in iterative nonlinear NMI. Williamson and Temperton (1981) still report a PMSL change by NMI of 4 mb at an unexceptional grid point over the USA.

In one case of nonlinear NMI applied to the operational model, the global rms change in PMSL was 1.0 mb with some extreme values of 3-6 mb. In this and other cases examined, the changes over data rich areas like Europe and the USA were nearly all less than 2 mb, with extreme values of 4 mb near the Rockies. Figure 10 gives an example difference chart for Europe.

Williamson, Daley and Schlatter (1981) found that NMI could make changes of up to 30m in 500 mb height in trough regions, with an rms change of 6m over a reasonably dense simulated observational network. They found rms wind differences at the same level to be 2-3 kt. Examples of corresponding difference fields for the operational model are shown in Figures 11 and 12, where height changes are limited to about 10m and wind differences to 4 kt.

Direct comparison of the increments obtained with the operational model with those published is difficult because the models and analysis schemes used are not identical. However, the balance obtained by repeated insertion is probably responsible for the relatively low PMSl increments obtained with the operational model. Surface pressure oscillations are linked mainly to the external mode which is effectively damped by the repeated insertion. The limited evidence also suggests that extreme height increments introduced by NMI are smaller with the repeated insertion method than with a standard statistical interpolation analysis. Wind increments would appear to be of the same order. They also increase with height, maximum 250 mb increments tending to be twice those at 500 mb. As we have seen in the jet stream case studies, NMI increments are required to remove modes of period around 12 hours which cannot be effectively damped by repeated insertion.

5. A measure of balance in normal mode space

In a balanced model state the time rate of change of gravity wave amplitudes should be small. A measure of balance sometimes quoted in the literature is

$$\mathrm{Bal}_m = \sum \left|\frac{dg}{dt}\right|^2$$

where g is the amplitude of a gravity mode in normal mode space and the sum is over all modes with vertical index m. The smaller the value of Bal, the closer the data are to the required balance.

Figure 13 shows typical values of Bal_m (m=1,5) for an operational analysis and the values after 1 and 2 iterations of NMI applied to that analysis. It is seen that 1 iteration reduces the noise level as measured by Bal by about a factor of 10 for all 5 modes. The extra improvement after a second iteration is minor. (Eigenvectors associated with different vertical modes are not in general orthogonal and so one cannot compare values of Bal for different m).

Williamson and Temperton (1981) and Errico (1984) report Bal for analyses produced by statistical interpolation without dynamic initialization. Their results show a reduction in Bal for the first 3 vertical modes by a factor of 50-100 after 1 iteration of NMI on the uninitialized data. The further reduction after a second iteration was about a factor of 10, with only small extra benefit with a third iteration. This suggests, therefore, that the operational assimilation produces an analysis with a balance roughly as good as that obtained by applying 1 iteration of nonlinear NMI to an uninitialized analysis.

An early method of dynamic initialization was that of forward and backward integration about the analysis time using a modified Euler backward time stepping scheme with damping properties (Nitta, 1969). Williamson and Temperton (1981) show that this scheme reduces the noise in the first two vertical modes. The values of Bal after 6 hours of this dynamic initialization are still about 10 times those obtained with 1 iteration of NMI on the uninitialized data or, by implication, with the present operational assimilation. This demonstrates the superiority of repeated insertion with divergence damping over the forward-backward scheme.

NMI is potentially useful when assessing analysis differences in forecast model intercomparison experiments. For example, ECMWF analyses must be interpolated in the vertical and the fields adjusted to new orography before a forecast with the operational model can be run from them. This interpolation may degrade the analysis and in particular its balance. This was demonstrated by comparing values of Bal for an operational analysis and one that had been converted to ECMWF grid point format and then interpolated back to the grid of the operational model.

The value of Bal_1 (external mode) was 5 times as large for the interpolated analysis, though for modes 2-5 the increase was less than 50%. In looking at the fine detail of analysis differences, it would be best therefore to compare only datasets which have undergone the same interpolation process. Application of NMI to these interpolated analyses could also help separate analysis differences into balanced and unbalanced components.

6. Conclusion

The results of Section 2 on quality control imply that introduction of NMI to the operational suite for that purpose would not be worthwhile. Dickinson and Gange (1985) also conclude that there are computationally more efficient ways to reduce the noise in the fine mesh model than NMI of the hemispheric forecast supplying the boundary data. From Section 5 it emerges that, by one measure of balance, the operational assimilation is about as effective as one iteration of nonlinear NMI on an uninitialized analysis. While it appears to have no place in the present operational suite, NMI has been found useful in diagnosing balance in the global model and will be helpful in assessing future changes to the operational analysis system.

Appendix - Computational Aspects of NMI

1. Creation of Normal Modes

The procedure of NMI is carried out in two stages. First one must solve for the normal modes of the model linearised about some basic state. Only a brief outline is given here. A fuller account is given by Temperton and Williamson (1981) and Daley (1981).

Separation of variables in the linearised equations of motion yields a vertical structure equation and a horizontal structure equation. Both depend on the particular space and time discretization of the model. One obtains the shallow water equations for the horizontal variation of each vertical mode which has an associated equivalent depth H. There is then one horizontal eigenvalue problem for each H, which can be transformed by Fourier analysis to an equation involving only time and latitude. The eigenvalues are related to the frequencies of the normal modes and the eigenvectors to the latitudinal structure. The modes can be classified according to frequency into slow Rossby modes and fast gravity modes. This analysis is only valid for global models with no lateral boundary conditions.

Knowledge of the equivalent depths for a particular model can be useful in interpretation of imbalances in that model. Table 1 gives the value of H, one for each σ level, for the operational global model linearised about an isothermal basic state of 300K (NMI is insensitive to the details of the basic state). Also tabulated are the corresponding phase speeds of the gravity waves on a non-rotating Earth, $\sqrt{gH}$. In practice, only the first 5 vertical modes are relevant for the NMI program which does not converge for higher internal modes. Reasons for this divergence are discussed in the references cited above.

Table 1

Model Level	Equivalent depth H (m)	Phase speed, $(gH)^{1/2}$ ms^{-1}
1	11862	341
2	3263.1	179
3	893.8	94
4	346.6	58
5	167.3	40.5
6	88.54	29.5
7	47.92	21.7
8	27.03	16.3
9	15.06	12.2
10	8.316	9.0
11	4.144	6.4
12	1.976	4.4
13	0.8452	2.9
14	0.2738	1.6
15	0.0392	0.6

2. Performing NMI

In the second step, grid point data are expanded in normal mode space, the coefficients in the expansion are modified and then the new data are transformed back to grid point space. If we write g for the coefficient in normal mode space of a particular gravity mode, its evolution equation is

$$\frac{dg}{dt} = - i \nu g + N \tag{1}$$

where ν is the eigenvalue associated with the mode and N is the combination of all the nonlinear terms transformed into normal mode space. In linear NMI, one simply neglects N and sets g=0 to suppress the fast oscillations. The NMI program used in the present experiments employs the Machenhauer version of nonlinear NMI, an iterative process described by

$$g_{j+1} = \frac{N_j}{i\nu} \tag{2}$$

so that the time tendencies of the gravity modes converge to zero. N_j is a function of the initial (and unmodified) Rossby mode coefficients r_o and the gravity mode coefficients at the jth iteration g_j.

In the NMI code, it is not necessary to compute the nonlinear terms N explicitly. Instead, the change in the coefficients g is computed over a short forecast (currently two time steps of Δt = 10s) and the linear part is subtracted off. The normal mode increments at each iteration are then given by

$$\Delta g = g_{j+1} - g_j = - i\nu \frac{dg_j}{dt} \qquad (3)$$

The program consists of 3 main routines. The first transforms the time derivatives of the grid point fields into vertical normal mode space, giving the right hand side of (3) in the form of horizontal arrays. Secondly, these time tendencies are transformed into horizontal normal mode space and horizontal fields of increments computed. Finally these are inverted to give grid point increments, ready for the next iteration.

The quantity Bal_m discussed in Section 5 is calculated at each iteration by summing over the time tendencies of the gravity modes with vertical index m.

$$Bal_m = \sum \left|\frac{dg}{dt}\right|^2 \qquad (4)$$

Its decrease after successive iterations gives a measure of the convergence of the NMI. The present NMI program initializes horizontal modes of all frequencies for a given vertical mode but a frequency cut off could be incorporated if desired. The initialization is adiabatic in that 'physics' routines are switched off during calculation of mode time tendencies.

In terms of computational resources, NMI is fairly expensive. The file presently holding the normal mode coefficients occupies space equivalent to 12 forecast datasets. Computation time on the CYBER for a nonlinear NMI with 2 iterations is roughly 5-6 minutes. Of this time, half is taken up with transformations between grid point and normal mode space and manipulation of mode coefficients. The remainder is occupied in running the two time step model forecasts and converting between the 'fields' format of the forecast model data and the 'rows' format which is input to the NMI part of the program.

Acknowledgements

The normal mode initialization package was developed by C Temperton and T B Fugard. The author would like to acknowledge helpful discussions with A C Lorenc and R S Bell.

References

Barwell, B.R. and Lorenc, A.C.	1985	A study of the impact of aircraft wind observations on a large-scale analysis and numerical weather prediction scheme. Quart. J.R. Met. Soc. 111, 103-129.
Bell, R.S.	1985	The Data Assimilation Scheme. Operational Numerical Weather Prediction System. Documentation Paper No. 3.
Daley, R.	1981	Normal Mode Initialization. Rev. Geophys. Space Phys. 19, 450-468.

Dickinson, A. and Gange, M.	1985	Some examples of noise in fine-mesh pressure and precipitation forecasts. Met O 11 Working Paper No. 82.
Errico, R.M.	1984	Convergence Properties of Machenhauer's Initialization Scheme. Mon. Wea. Rev. 111, 2214-2223.
Nitta, T.	1969	Initialization and analysis for the primitive equation model. Proc. WMO/IUGG Symposium on Numerical Weather Prediction, Tokyo, pp VI, 11-20, Japan Meteor. Agency.
Temperton, C. and Williamson, D.L.	1981	Normal Mode Initialization for a Multilevel Grid-Point Model. Part I: Linear Aspects. Mon. Wea. Rev. 109, 729-743.
Williamson, D.L. and Temperton, C.	1981	Normal Mode Initialization for a Multilevel Grid-Point Model. Part II: Nonlinear Aspects. Mon. Wea. Rev. 109, 744-757.
Williamson, D.L. and Daley, R.	1983	A Unified Analysis - Initialization Technique. Mon. Wea. Rev. 111, 1517-1536.
Williamson, D.L., Daley, R. and Schlatter, T.W.	1981	The Balance between Mass and Wind fields resulting from Multivariate Optimal Interpolation. Mon. Wea. Rev. 109, 2357-2376.

<u>Figure Captions</u>

1. Spatial mean jet momentum (arbitrary units) as a function of time. (Operational run, data time 0Z, 2/6/84). The quantities plotted are averaged over a latitude/longitude area enclosing the jet and over model levels 10-12 ($\sigma = 0.31$ to $\sigma = 0.19$). The model time step is $\Delta t = 15$ minutes. +++: modulus of momentum, □□□□ : u component, ▲▲▲▲ = v component.

2. As for Figure 1 but with 1 iteration of NMI on 5 vertical modes.

3. Amplitude of oscillation in mean v wind component of jet (data time 0Z, 2/6/84) as a function of the number of vertical modes initialized for 1 iteration of NMI. The amplitude is measured by v(t+4 hours) - v(t+o), appropriately scaled.

4. Operational analysis of 250 mb height (0Z, 2/6/84).

5. Difference field of u wind component (kt) at 250 mb (0Z, 2/6/84); uninitialized - NMI analysis.

6. Mean jet kinetic energy as a function of time. (data time: 6Z, 15/1/85) Model timestep $\Delta t = 15$ minutes. □□□ Uninitialized run ——NMI.

7. Mean jet momentum as a function of time. (Data time 6Z, 20/7/85). Values plotted each timestep are for uninitialized run, key as in 1 above. The solid lines show the u and v components in the NMI run.

8. Difference fields of u wind component (kt) for t+8 forecasts from uninitialized and initialized analyses valid 6Z, 20/7/85; uninitialized - NMI analysis.

9. As for 1 above, except data time 6Z, 26/8/85.

10. PMSL difference chart (uninitialized - NMI analysis) for 6Z, 20/7/85.

11. As in 10 for 500 mb height field.

12. As in 10 for u wind component at 500 mb.

13. Values of Bal for the first 5 vertical modes after 0, 1 and 2 iterations of NMI on an operational analysis. Data time: 6Z, 10/5/85.

FIGURE 1

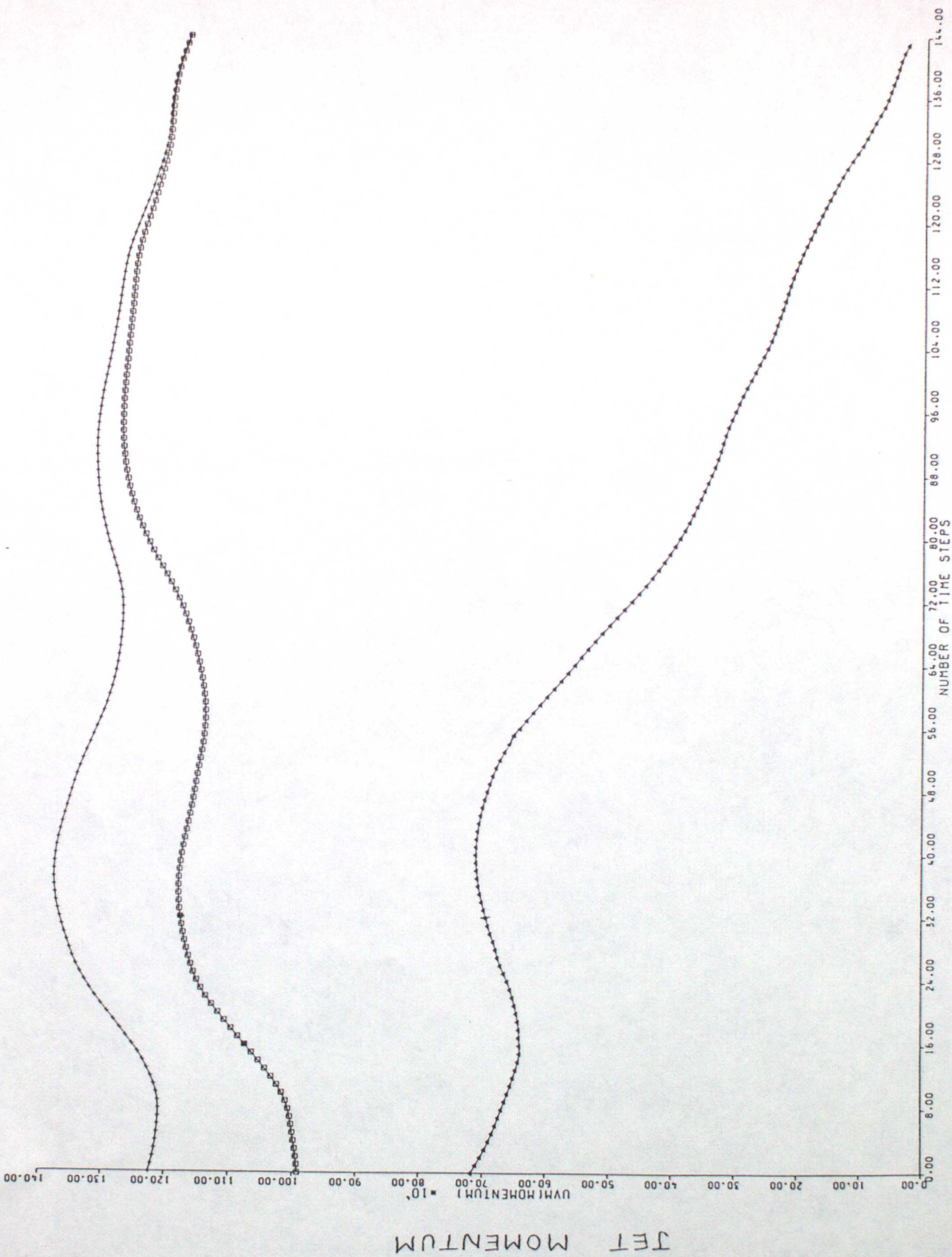
JET MOMENTUM
UVM(MOMENTUM) *10
NUMBER OF TIME STEPS
0.00
10.00
20.00
30.00
40.00
50.00
60.00
70.00
80.00
90.00
100.00
110.00
120.00
130.00
140.00
8.00
16.00
24.00
32.00
40.00
48.00
56.00
64.00
72.00
80.00
88.00
96.00
104.00
112.00
120.00
128.00
136.00
144.00

FIGURE 2

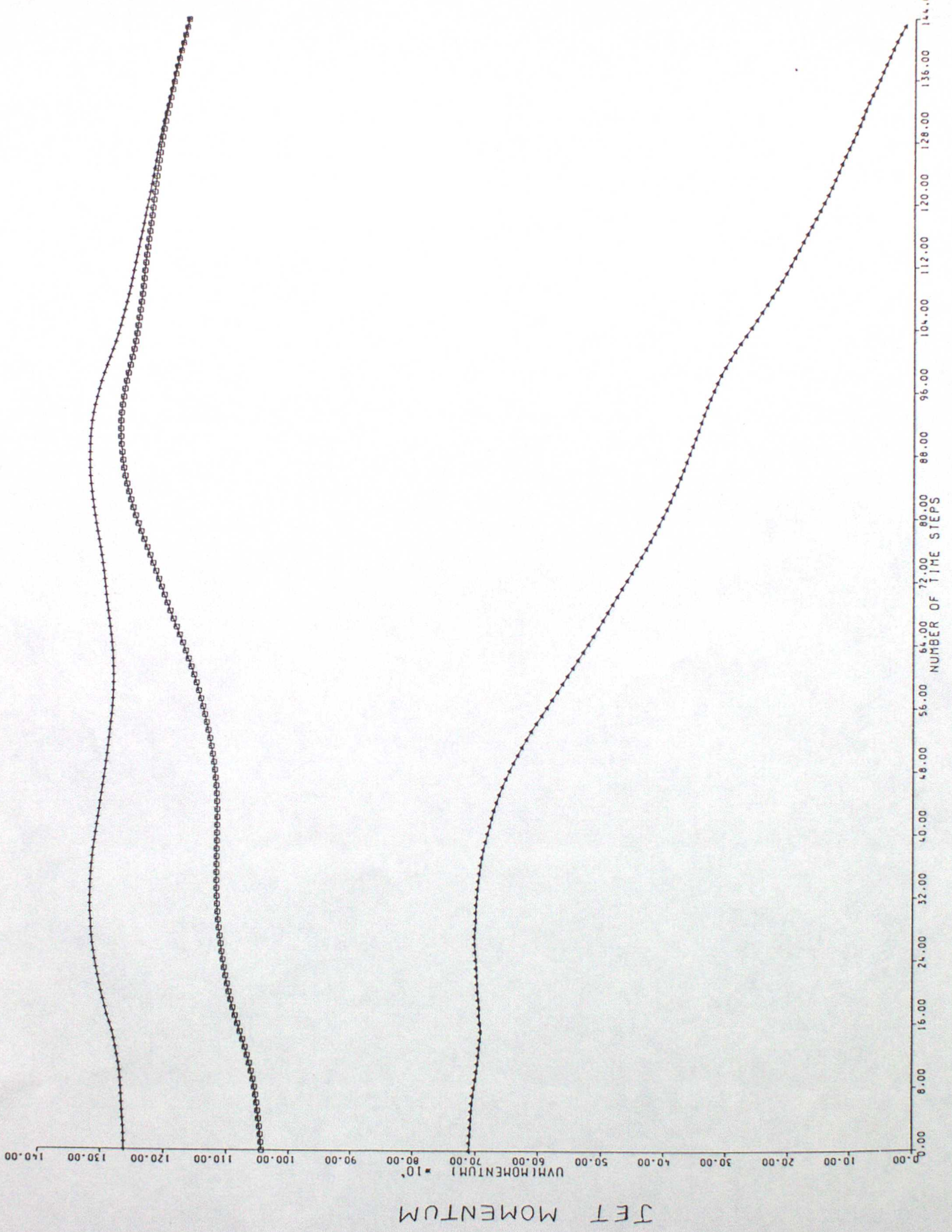
JET MOMENTUM
NUMBER OF TIME STEPS
0.00
8.00
16.00
24.00
32.00
40.00
48.00
56.00
64.00
72.00
80.00
88.00
96.00
104.00
112.00
120.00
128.00
136.00
144.00
0.00
10.00
20.00
30.00
40.00
50.00
60.00
70.00
80.00
90.00
100.00
110.00
120.00
130.00
140.00

FIGURE 3

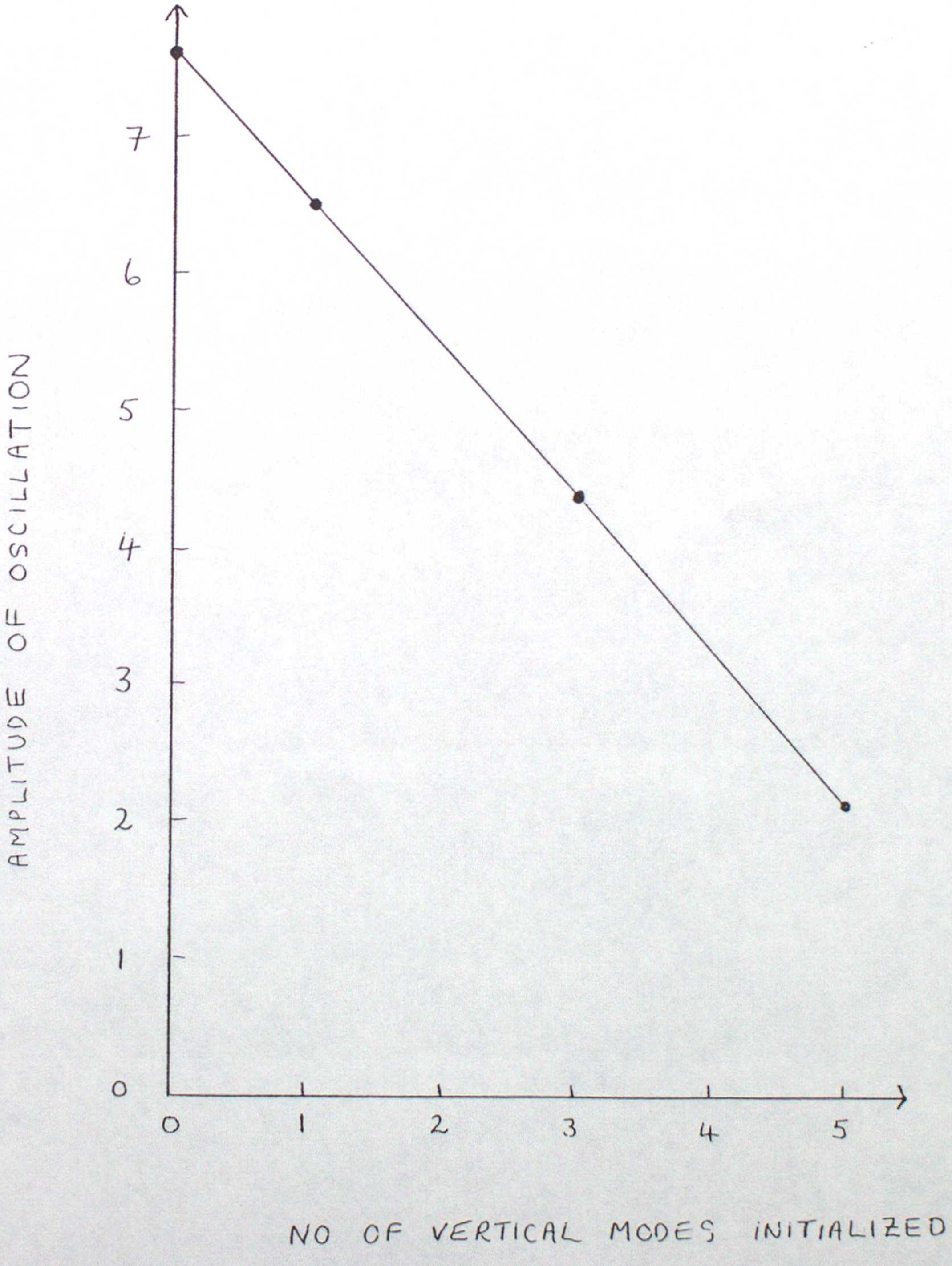
AMPLITUDE OF OSCILLATION
7
6
5
4
3
2
1
0
0
1
2
3
4
5
NO OF VERTICAL MODES INITIALIZED

FIGURE 4

UNINITIALISED
VALID AT 0Z ON 2/6/1984 DAY 154   DATA TIME 0Z ON 2/6/1984 DAY 154
LEVEL: 250 MB

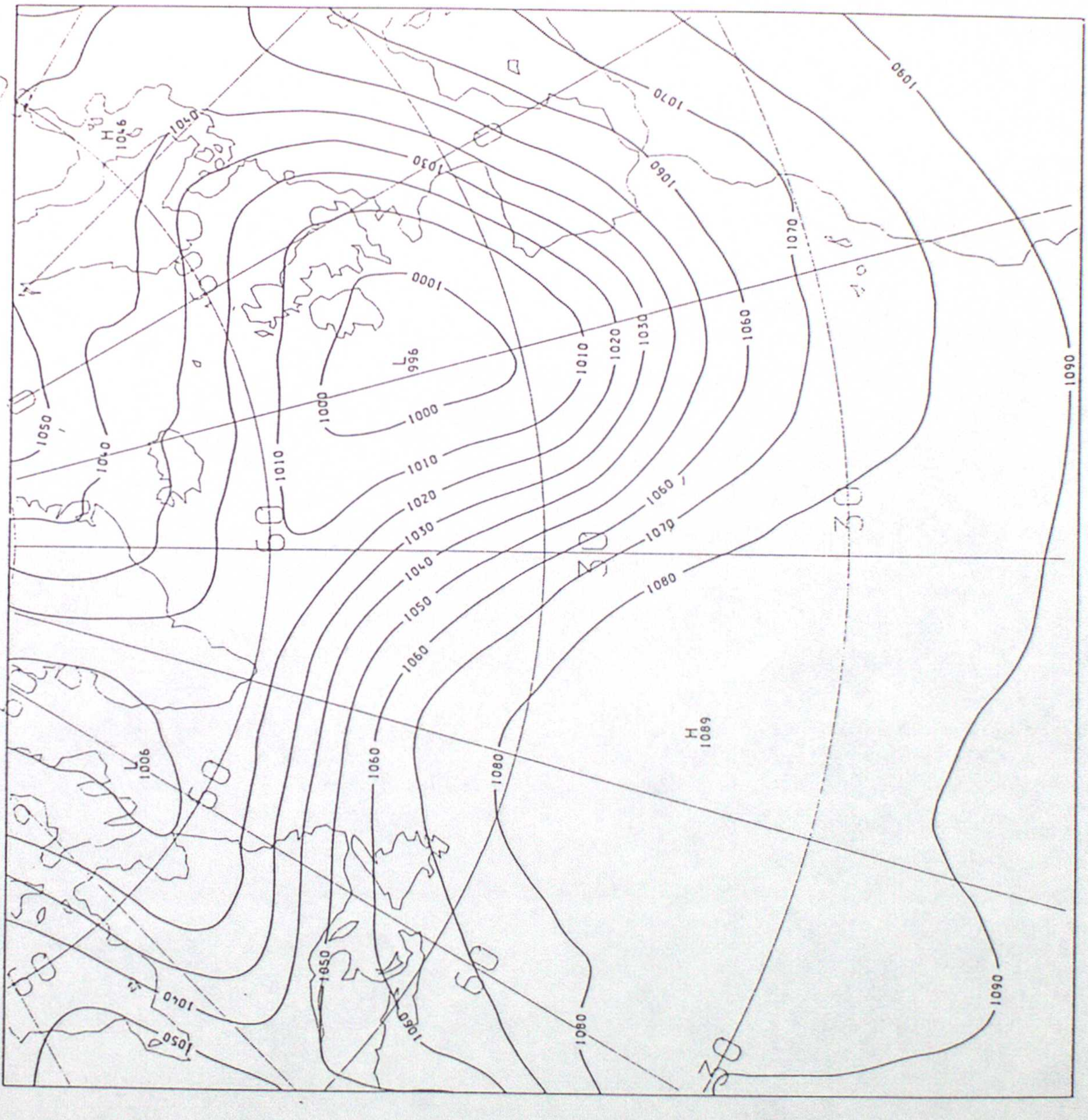

FIGURE 5

U WIND DIFFERENCE
VALID AT 0Z ON 2/6/1984 DAY 154 DATA TIME 0Z ON 2/6/1984 DAY 154
LEVEL: 250 MB

FIGURE 6

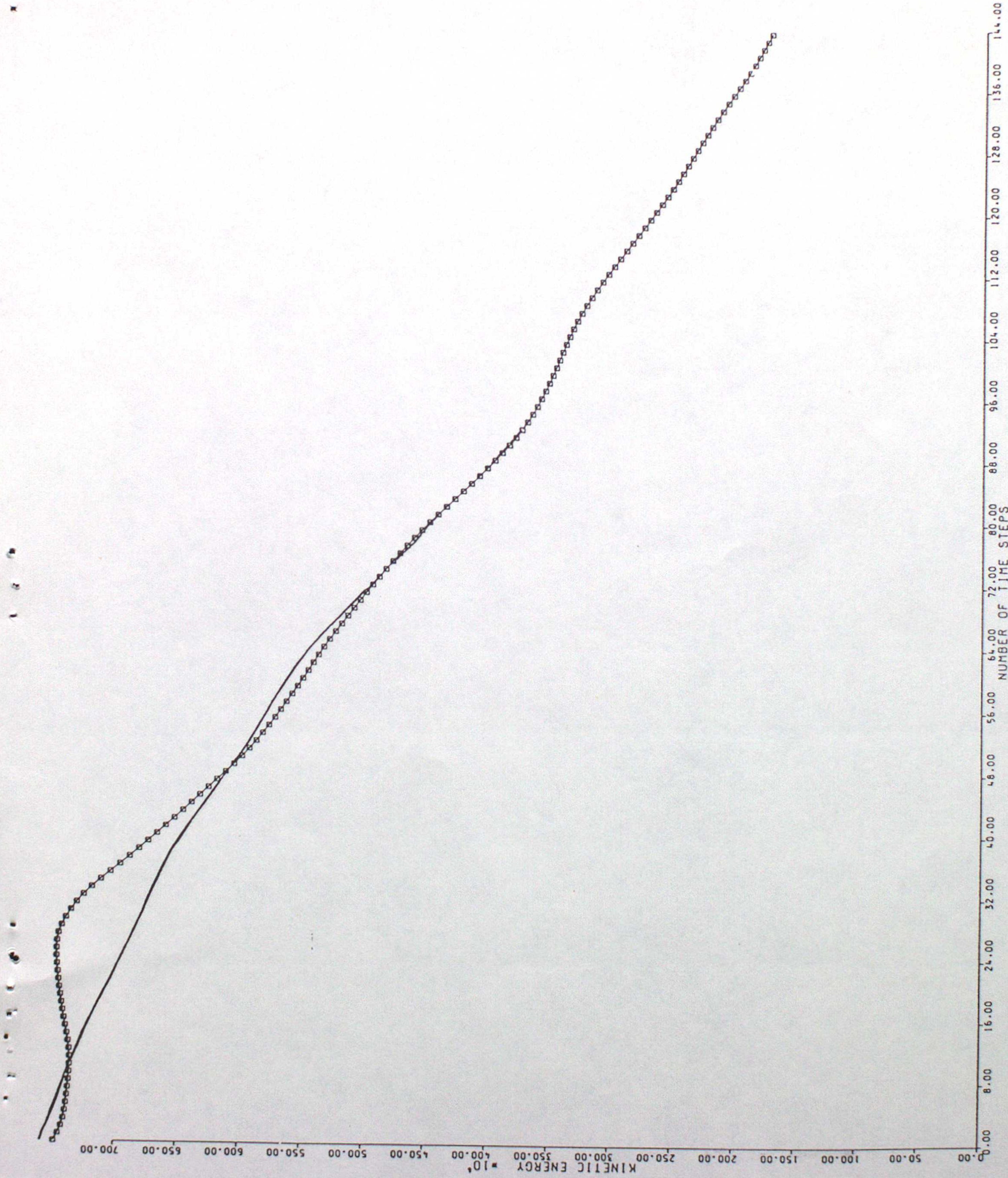
KINETIC ENERGY *10^1
0.00
50.00
100.00
150.00
200.00
250.00
300.00
350.00
400.00
450.00
500.00
550.00
600.00
650.00
700.00
NUMBER OF TIME STEPS
0.00
8.00
16.00
24.00
32.00
40.00
48.00
56.00
64.00
72.00
80.00
88.00
96.00
104.00
112.00
120.00
128.00
136.00
144.00

FIGURE 7

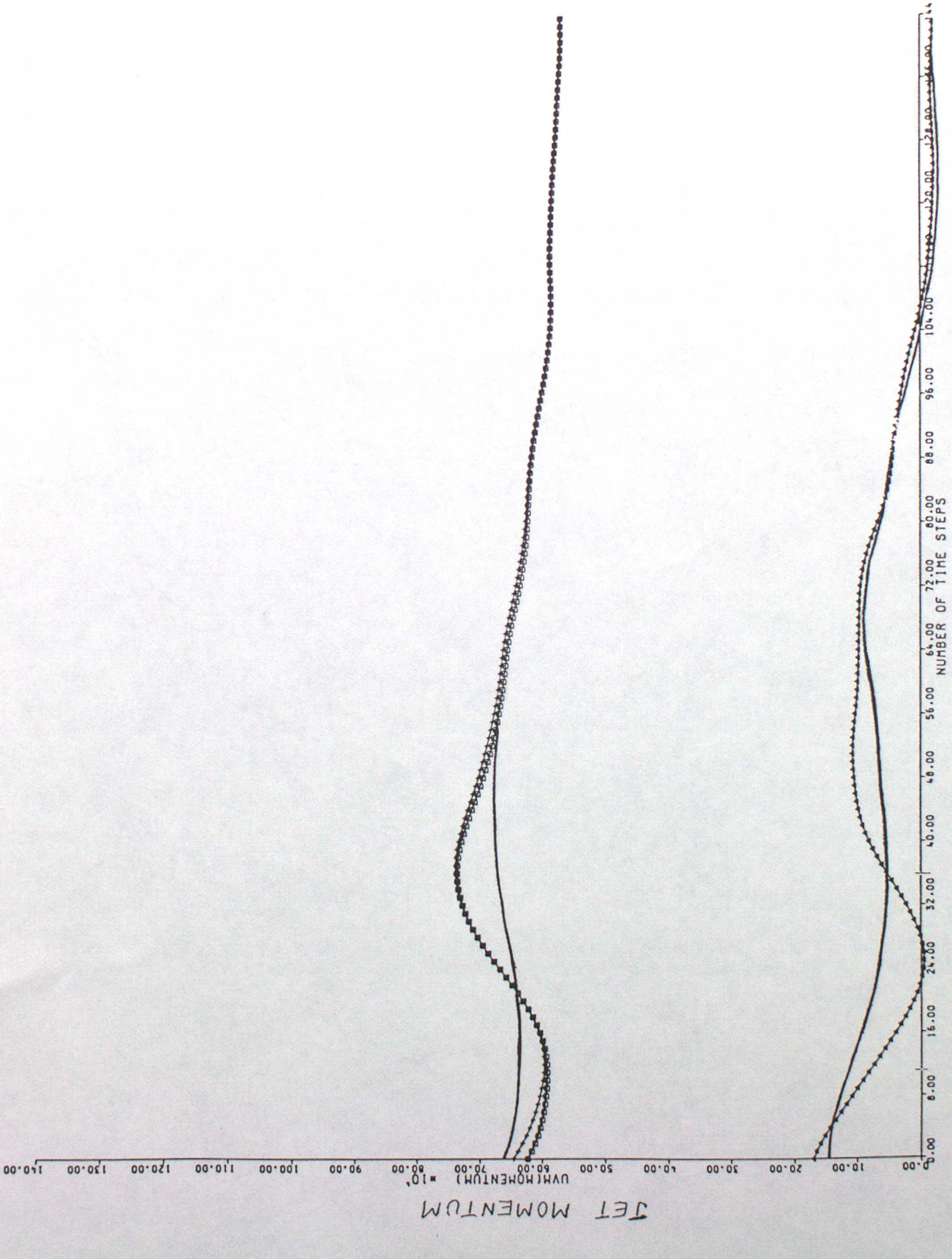
JET MOMENTUM
UVM(MOMENTUM) *10'
NUMBER OF TIME STEPS
0.00
8.00
16.00
24.00
32.00
40.00
48.00
56.00
64.00
72.00
80.00
88.00
96.00
104.00
112.00
120.00
128.00
136.00
144.00
10.00
20.00
30.00
40.00
50.00
60.00
70.00
80.00
90.00
100.00
110.00
120.00
130.00
140.00

FIGURE 8

U WIND DIFFERENCE
VALID AT 14Z ON 20/7/1985 DAY 201 DATA TIME 6Z ON 20/7/1985 DAY 201
LEVEL: 250 MB

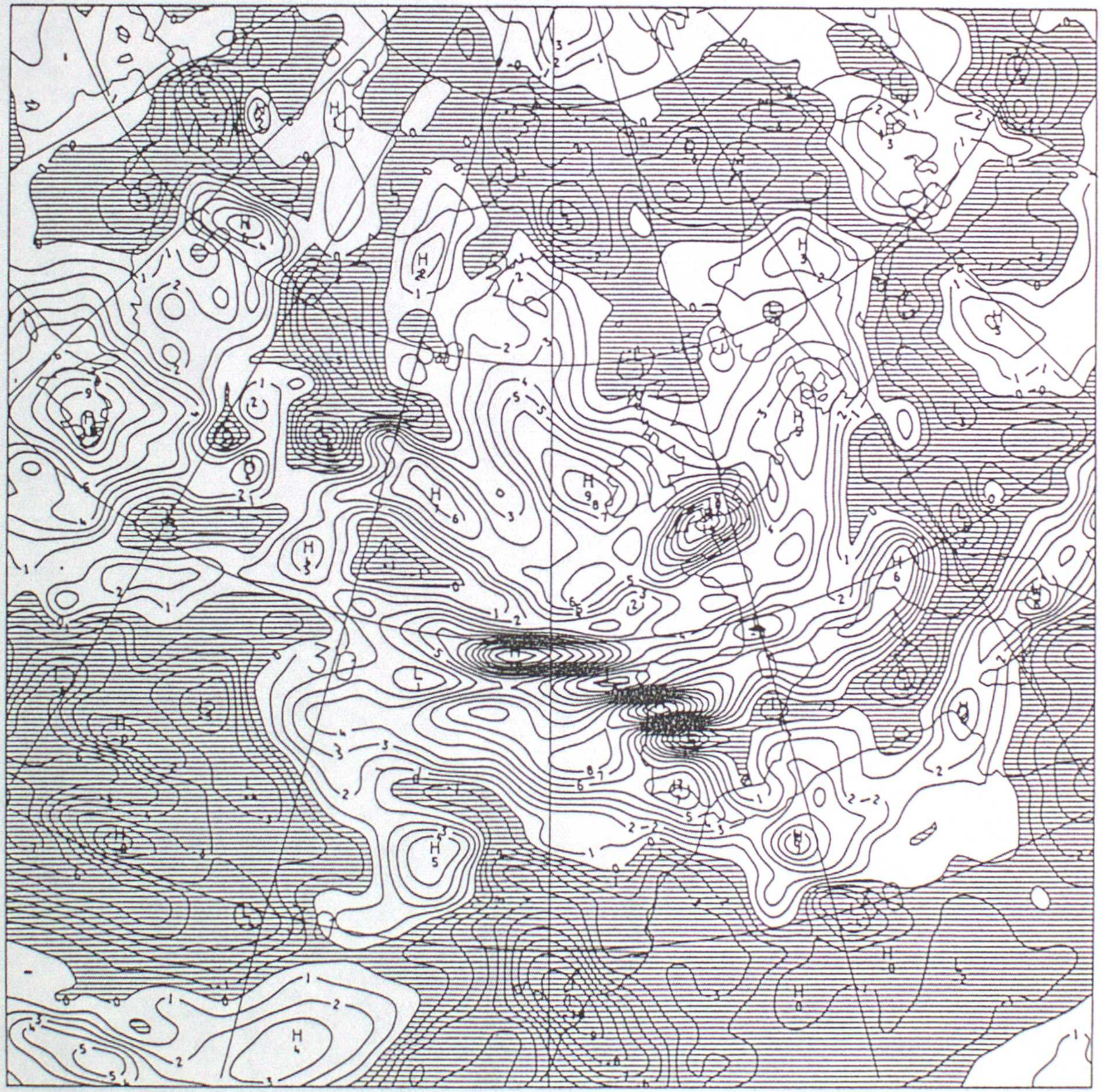

FIGURE 9

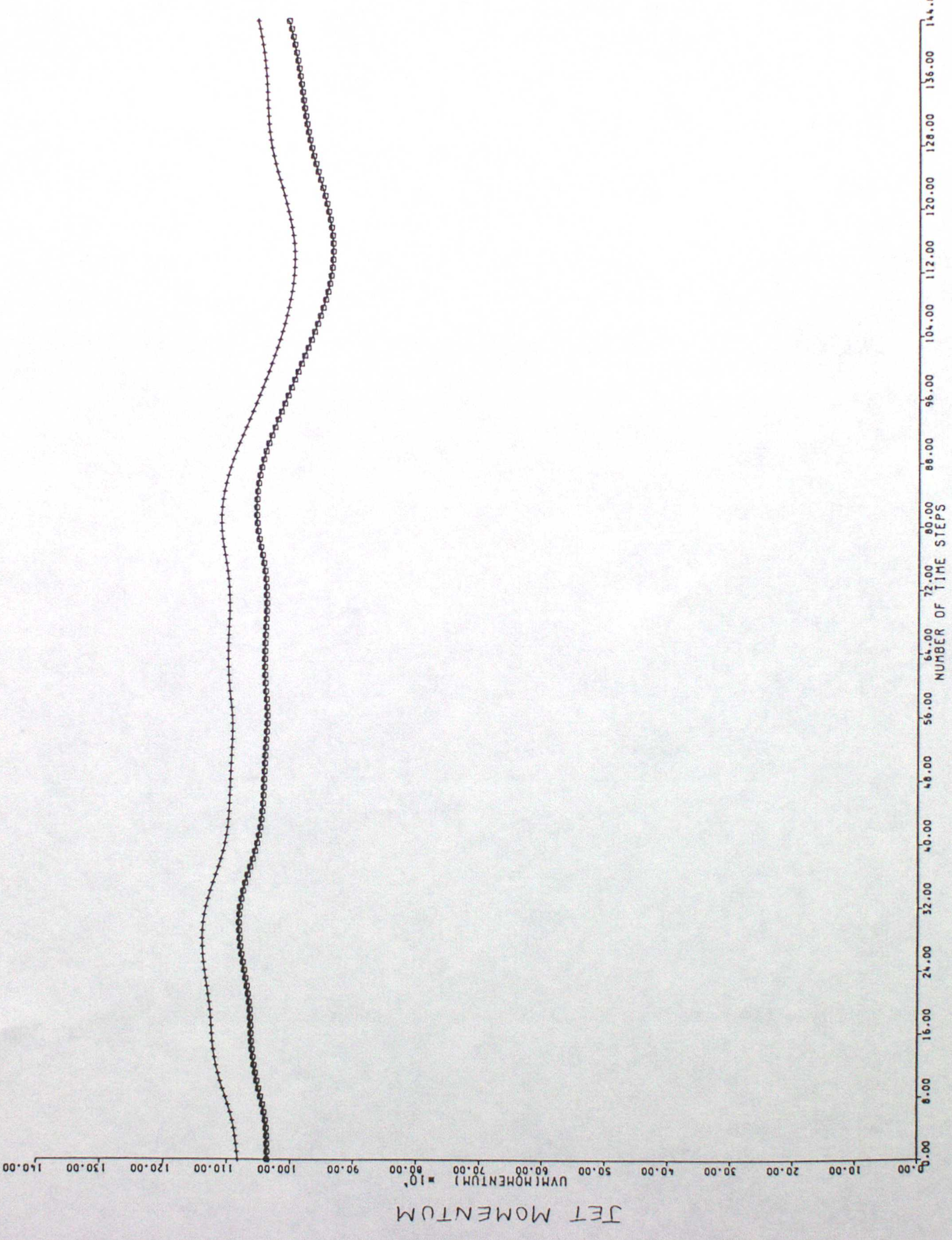

JET MOMENTUM

FIGURE 10

MSLP DIFFERENCE
VALID AT 6Z ON 20/7/1985 DAY 201 DATA TIME 6Z ON 20/7/1985 DAY 201
LEVEL: SEA LEVEL

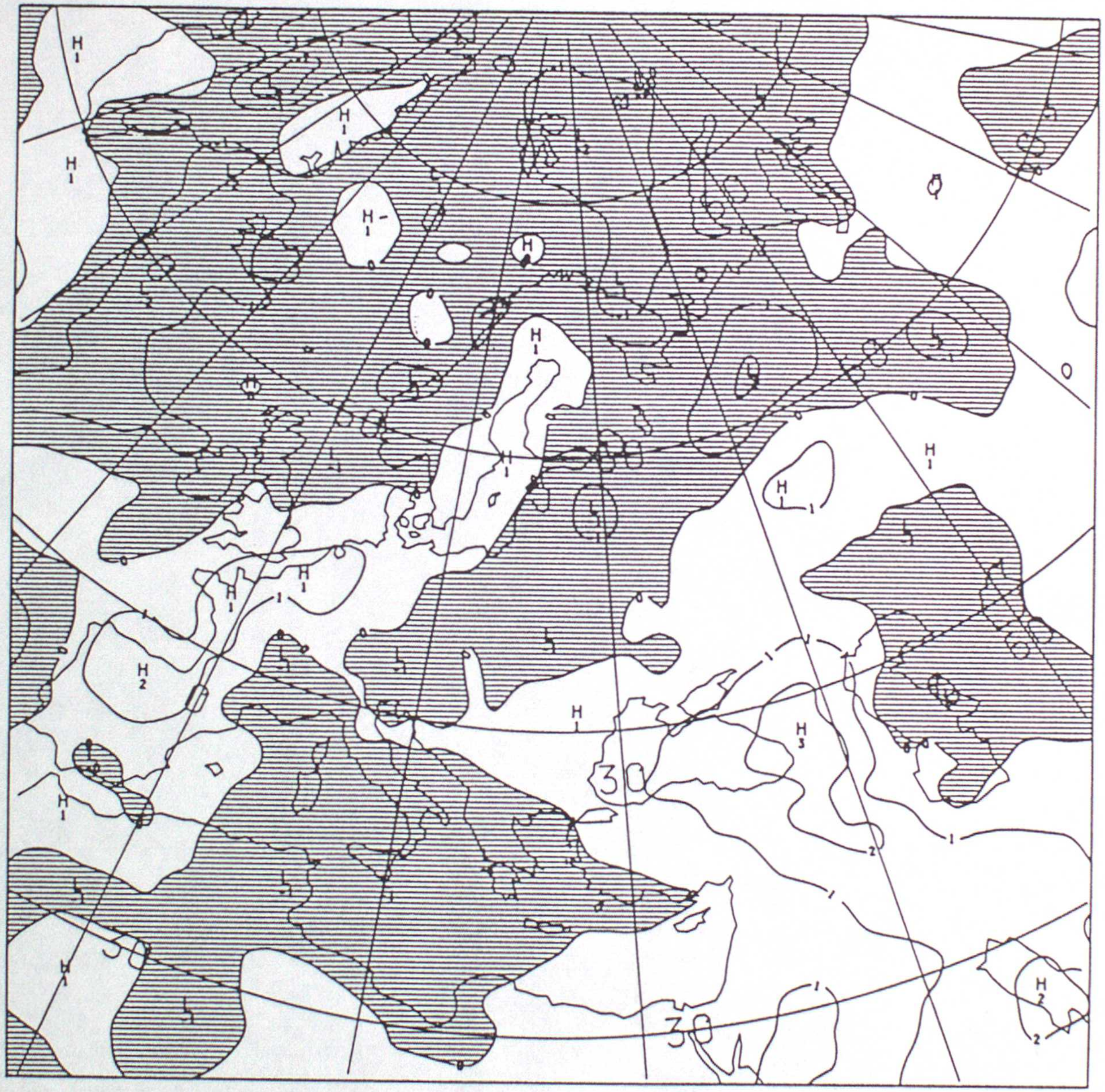

HEIGHT DIFFERENCE
VALID AT 6Z ON 20/7/1985 DAY 201 DATA TIME 6Z ON 20/7/1985 DAY 201
LEVEL: 500 MB

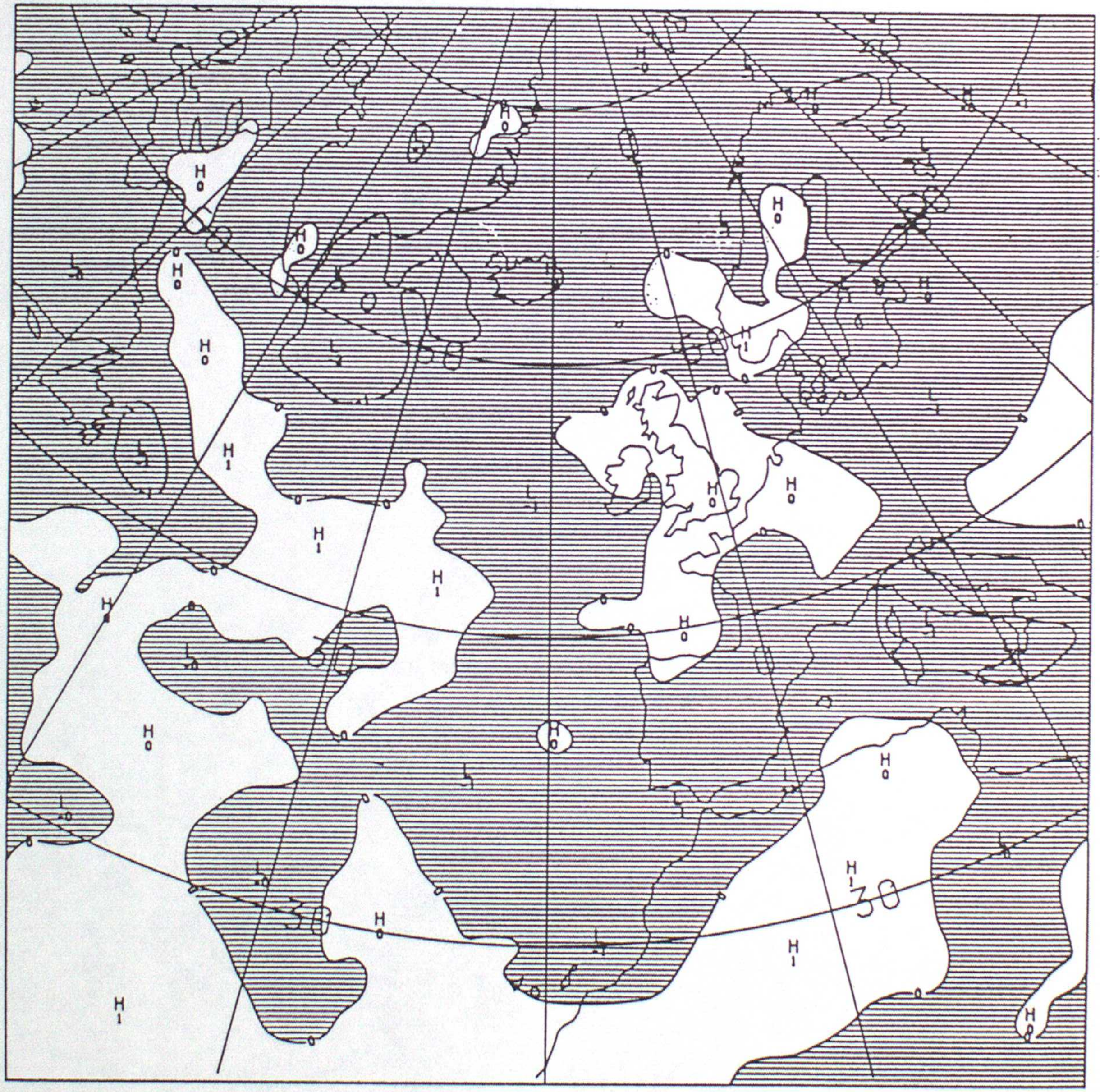

FIGURE 11

U WIND DIFFERENCE
VALID AT 6Z ON 20/7/1985 DAY 201 DATA TIME 6Z ON 20/7/1985 DAY 201
LEVEL: 500 MB

FIGURE 12

FIGURE 13